# Project Assignment 1

Colin Fricke, Nathan Vairora,
Sai Srinivas Tatwik Meesala

RAS 557: Foldable Robotics

Dr. D. Aukes

October 15 2025

Fall 2025

# Table of Contents

# Table of Figures



# Table of Tables

# 1. Team Goals

## *1.1. Candidate Identification*

The team will focus on the geometrid inchworm (Manduca sexta) as the biological model for this project. The inchworm's looping, anchor-and-drag gait involves sequential gripping and releasing of its anterior and posterior prolegs, producing an alternating contraction and extension of its flexible body. This motion can be replicated mechanically as a lift-and-drag mechanism combining vertical lifting and horizontal translation phases.

The robotic analog will use two rigid gripping pads joined by planar linkages that perform both extension and elevation. The lift motion will be achieved by a prismatic linkage, while the horizontal translation will be implemented through a Sarrus-type four-bar coupler system. This configuration allows replication of the biological inchworm's characteristic gait using rigid linkages suitable for MuJoCo simulation and laser-cut foldable construction.

## *1.2. Intent of Choice*

Inchworms offer a simple yet efficient form of terrestrial locomotion based on friction modulation rather than wheels or legs. Prior studies [3, 4, 5] show that inchworm-type robots achieve large stride-to-body-length ratios with minimal actuation complexity. However, most prior prototypes rely on smart materials (e.g., Shape Memory Alloy (SMA) wires) that obscure the quantitative relation between geometry, stroke amplitude, and performance.

This project's intent is to construct a simplified rigid-link prototype that isolates geometric and kinematic parameters from material behavior. By modeling the system with MuJoCo, the team can vary link lengths, hinge damping, and actuation displacement to study how these factors affect stride length, lift height, and energy efficiency. The outcome will be a reproducible, foldable crawler that quantitatively connects linkage design to gait performance.

## *1.3. Research Question Rationale*

- Scope

  To ensure feasibility within one semester, the study will focus on a single planar lift–drag motion of an inchworm-inspired crawler scaled to 100 mm body length. The robot will consist of five rigid links with one linear actuator representing the muscular contraction phase. Only horizontal

crawling on a flat substrate will be modeled, neglecting climbing or turning. Materials will be restricted to cardstock and 3D-printed joints to remain compatible with foldable fabrication techniques introduced in class. Simulation and optimization will be conducted in MuJoCo with Python.

- Impact

Small terrestrial crawlers are useful for inspection, environmental sensing, and confined-space exploration where wheels fail. Inchworm-based mechanisms provide high traction with low slip due to friction modulation ($\mu_{anchor} \approx 0.9$, $\mu_{slide} \approx 0.3$). Such systems are increasingly relevant for soft and deployable robotics, as highlighted in [6]. The analytical framework from [3] can now be combined with rigid-body simulations to generate measurable data for design optimizations, something that was not computationally accessible a decade ago. Broader impacts include modular crawling modules that can be embedded in origami or foldable structures for field-deployable robotics.

- Team Fit

Each team member contributes complementary expertise:

- Linkage synthesis and CAD modeling.
- Python and MuJoCo simulation for kinematic and dynamic validation.
- Data processing and visualization for torque, power, and stride analysis.
- Collectively, these skills align with the learning goals of RAS 557: rigid and flexible mechanism design, vector-based modeling, and dynamic performance evaluation.

- Topic Fit

This research directly applies foldable-robotics concepts:

- Conversion of a biological continuum body into a planar four-bar–Sarrus hybrid linkage.
- Use of constraint-equation modeling and Jacobian analysis to relate input stroke to end-effector motion.
- Implementation and visualization through MuJoCo simulation of a foldable rigid-link mechanism

- Estimating actuator torque and mechanical power.

The inchworm's two-anchor gait exemplifies the foldable-robotics principle of transforming soft biological motion into compact, manufacturable, and analyzable mechanical systems.

# 2. Background Research

## *2.1. Existing Papers*

The team searched for the primary biomechanics of Manduca sexta crawling and inchworm-style robotic counterparts. Four core sources anchor this review: (1) 3D kinematics of Manduca crawling, (2) horizontal vs vertical gait kinematics, (3) ground-reaction forces (GRFs) during crawling, and (4) an inchworm/caterpillar-inspired robotic gait paper used widely in the field.

1. van Griethuijsen & Trimmer (2009, Journal of Experimental Biology) [1]
   This study provides the first full-body, 3-D kinematic dataset for Manduca sexta crawling on horizontal and vertical substrates. Average larval mass was 2.05 ± 0.14 g. Stride cycles were divided into stance and swing phases for each proleg pair. The authors found that the sequence and timing of proleg engagement were nearly identical across orientations, implying that the underlying control is largely orientation independent. This validates the use of a planar two-anchor gait model for simulation. Mean stride period ≈ 2.8 s and center-of-mass translation ≈ 30% body length per cycle give a baseline stride length of roughly 15 to 20 mm for a 60 mm larva, metrics directly transferable to the design targets in MuJoCo.

2. Lin and Trimmer (2010 / 2011 corrigendum, Journal of Experimental Biology) [2]
   Lin and Trimmer constructed a multi-contact force plate to measure ground-reaction forces (GRFs) beneath each proleg. They demonstrated that anterior prolegs generate forward thrust primarily through tensile pulling, while posterior prolegs often apply drag forces during body extension. Vertical loads were distributed nearly evenly among abdominal prolegs during stance. These findings inform the mechanical anchor sequencing in the crawler: front grip pulls (low friction), rear grip anchors (high friction). The reported friction ratios between sliding and anchoring phases ($\mu_{slide} \approx 0.3$, $\mu_{anchor} \approx 0.9$) define quantitative limits for selecting surface materials and setting MuJoCo friction parameters.

3. Plaut (2015, International Journal of Non-Linear Mechanics) [3]
   Plaut formulated a mathematical model describing the inchworm body arch as a flexible beam undergoing large deflection. The model yields

closed-form relations linking curvature, arc length, and forward displacement per cycle. For small-amplitude bending,

$$strain \approx \frac{1}{2} \cdot L \cdot \theta^2$$

where θ is the mid-body deflection angle and L is the body length. This result constrains the target stroke amplitude of the mechanical linkage. By matching the simulated lift height (~10 % body length) to Plaut's derived curvature limits, the team ensures biological plausibility in the rigid model's deformation envelope.

4. Wang et al. (2009, Progress in Natural Science) [4]
   This paper introduces a mini-modular climbing caterpillar robot that implements alternating anchor–release motion through a variable-length linkage chain. Each module contains one driving motor and two passive joints, creating a continuous sequence of contraction and extension similar to the Manduca sexta gait. Reported stride length ≈ 14 mm, frequency ≈ 0.35 Hz, and average speed ≈ 5 mm $s^{-1}$. The mechanical design demonstrates that a rigid, linkage-based system can successfully reproduce inchworm-style locomotion using discrete joints rather than soft deformation, making it the closest engineering analog to the lift-and-drag specification.

5. Li et al. (2024, An Inchworm-Like Climbing Robot Based on Cable-Driven Grippers) [5]
   Li and colleagues developed a cable-driven climbing crawler capable of attaching and releasing alternately through two grippers. Their design realizes high payload-to-mass ratios (>2.5 × body weight) and efficient vertical mobility. The cable-driven actuation simplifies the integration of lightweight flexible joints. This reference demonstrates how actuation strategy affects the achievable stride-to-body-length ratio and suggests potential scaling strategies for foldable linkage systems.

6. Min Pan et al. (2025, Advanced Science) [6]
   Pan et al. reviewed bio-inspired mechanisms and actuation of soft robotic crawlers, classifying inchworm motion as a "two-anchor peristaltic mechanism." Their synthesis identifies key parameters like friction anisotropy, anchoring stability, energy efficiency, and adaptability, which form the principal design metrics for soft or foldable crawlers. They highlight how friction modulation and alternate anchoring enable efficient propulsion across complex surfaces. These principles define the system's

performance criteria: controllable friction ratio is > 2.5, stride ≈ 50 % body length, and cycle frequency ≈ 0.3–0.5 Hz.

7. Wu Fan (2024, A Kinematic Analysis of a Line Robot Based on Biomimicry of Inchworms) [7]
   Wu Fan proposed a line-inspection robot employing a bow-and-release motion identical to the inchworm's looping gait. The paper develops a complete slider-crank kinematic model that computes forward travel distance per half-rotation of the driving gear:
   $$l = \frac{2bz}{a}$$
   where b is the fore-arm length, z is the crank offset, and the link spacing. The theoretical running speed was ≈ 1.1 m $s^{-1}$, demonstrating scalability to larger rigid systems. The model provides direct guidance for setting the stroke length and hinge spacing in the linkage CAD.

## *2.2. Collecting Design Criteria*

Across these studies, Manduca sexta biomechanics and inchworm-style robots share the same core locomotion strategy, alternate anchoring, and body contraction driven by frictional asymmetry.

- Biological data define feasible ranges:
  - stride ≈ 0.5 L
  - cycle ≈ 2 to 3 s
  - and friction $\mu_{anchor} / \mu_{slide} \approx 3$.
- Analytical modeling [3][7] quantifies curvature and stroke relations for rigid analogs.
- Robotic implementations [4] validate mechanical feasibility using linkage or cable actuation.
- Soft-crawler reviews [6] highlight energy efficiency and material compliance as future directions.

These results converge into measurable design criteria for the foldable inchworm robot:

- Stride length ≈ 15 mm (half of body length).
- Lift height ≈ 5 mm (8 to 10 % of body length).
- Cycle frequency 0.3 to 0.5 Hz.
- Friction ratio μ_anchor: μ_slide ≥ 3:1.

- Payload ≥ 2× self-weight.

These quantitative and mechanical parameters define the benchmark for the subsequent Goal Performance Metrics section.

## *2.3. Key Information*

Biological inchworms of the family Geometridae use a two-anchor locomotion sequence that alternates between gripping and releasing their anterior and posterior prolegs. During each stride, the posterior segment anchors while the anterior lifts, extends, and reattaches before the rear detaches and follows through contraction. This produces a looping gait with a stride length approximately one-half of body length and a cycle period of about 2 to 3 seconds [3]. Ground-reaction measurements [2] indicate that peak contact forces reach roughly 1.5 times body weight during the anchor–slide transition, confirming that frictional asymmetry and coordinated timing are essential for efficient propulsion.

The body deformation during contraction can be modeled as a continuous elastic beam under large deflection, as described by [3]. The curvature κ and strain ε follow a relationship consistent with slender-beam bending, with

$$\kappa \approx \frac{\theta}{L}$$

and

$$\varepsilon \approx \frac{1}{2}(h\kappa)^2$$

where h is the body diameter. Typical larval curvatures remain below 0.1 $mm^{-1}$, limiting surface strain to less than 2 %. This natural limit constrains the geometric amplitude that should be replicated in mechanical analogs.

From an energetic perspective, the cycle work output of a 10 g larva is estimated between $10^{-4}$ and $10^{-3}$ J, giving an efficiency benchmark for small-scale crawling robots. Any artificial system operating within this energy envelope per stride can be considered biomimetically efficient.

In robotic analogs, the same kinematics can be reproduced using a two-anchor rigid-link mechanism driven by a single linear actuator or equivalent linkage motion. Each anchor pad alternates between high-friction (anchored) and low-friction (sliding) states, matching the biological tension–drag pattern observed in Manduca sexta. Maintaining link flexural rigidity $10^{-3} N \cdot m^2$ ensures the mechanism remains stiff enough to resist excessive bending while keeping curvature within biologically realistic bounds ($\kappa < 0.1\, mm^{-1}$).

The inchworm's locomotion acts as an open-chain system during extension and contraction, with one end free and the other fixed. In contrast, caterpillar-like variants intermittently form a closed-chain configuration when

both ends are anchored simultaneously. For accurate internal force prediction and actuator sizing, this dual state must be modeled using a four-link closed-chain representation in MuJoCo, allowing constraint-based evaluation of joint torques and reaction forces at each anchor.

These biomechanical and mechanical insights provide the quantitative framework for linking biological motion parameters, curvature, friction ratio, and energy cost to the foldable, linkage-based inchworm prototype.

## *2.4. Key Figures*

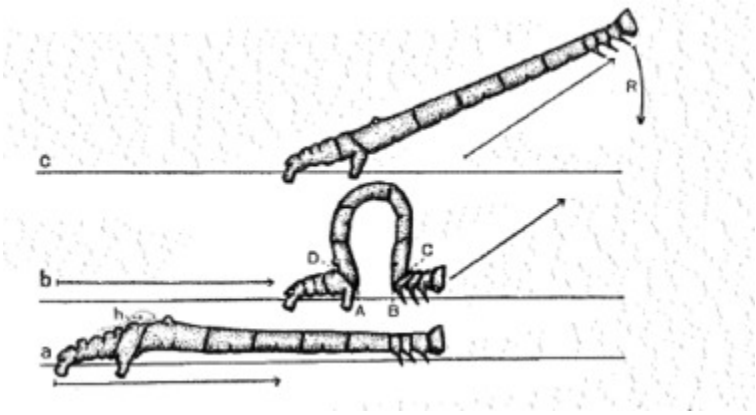


*Figure 1. Biological Reference: Beam-Bending Model of Inchworm Gait [3]*

This schematic shows the three sequential phases of inchworm locomotion.

- Rear anchor, front slide – posterior prolegs fixed, anterior extends forward.
- Front anchor, rear slide – anterior prolegs fixed, posterior contracts.
- Reset phase – body curvature returns to neutral as both ends reattach.

Plaut's model defines the relationship between beam curvature, strain energy, and net displacement ($\Delta x$), forming a quantitative foundation for the stroke amplitude and curvature constraints used in the mechanism design. This figure highlights how the inchworm converts asymmetric friction and cyclic bending into efficient forward motion.

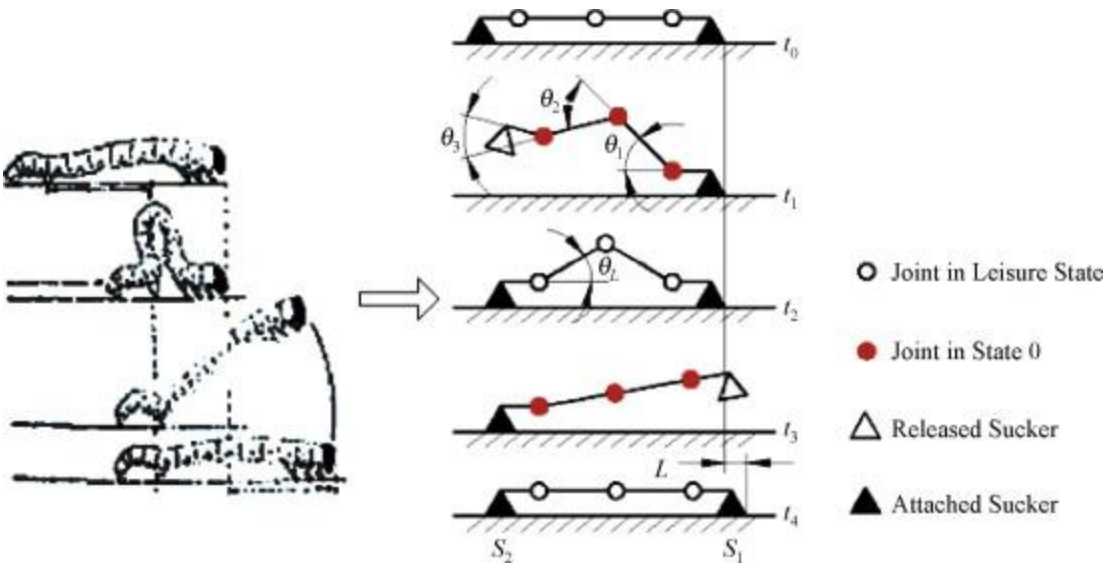


*Figure 2. The kinematics model and gait of an inchworm[4]*

The figure above depicts a four-link mini-modular caterpillar robot using alternating suction actuators to mimic inchworm anchoring. The figure shows the mechanical chain configuration corresponding to biological phases front anchor/rear slide and rear anchor/front slide, confirming that discrete rigid modules can approximate continuous larval motion.

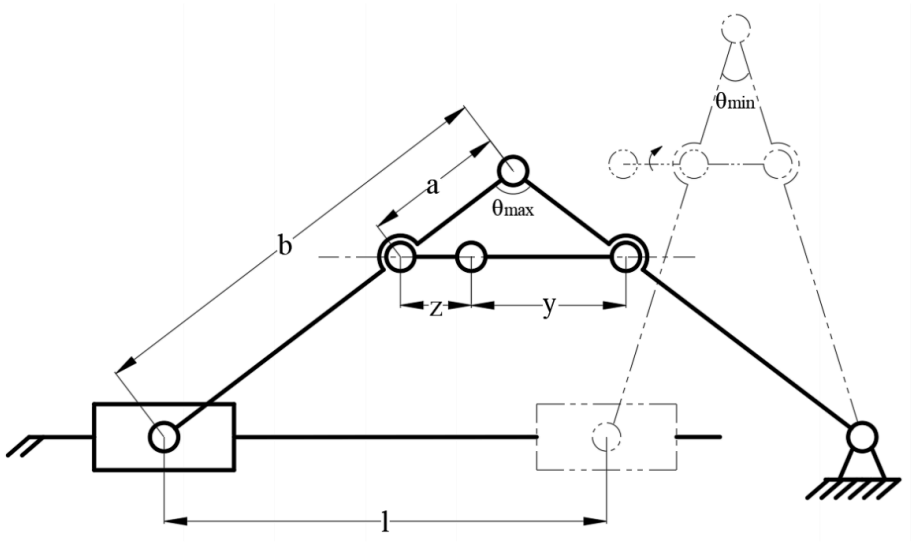

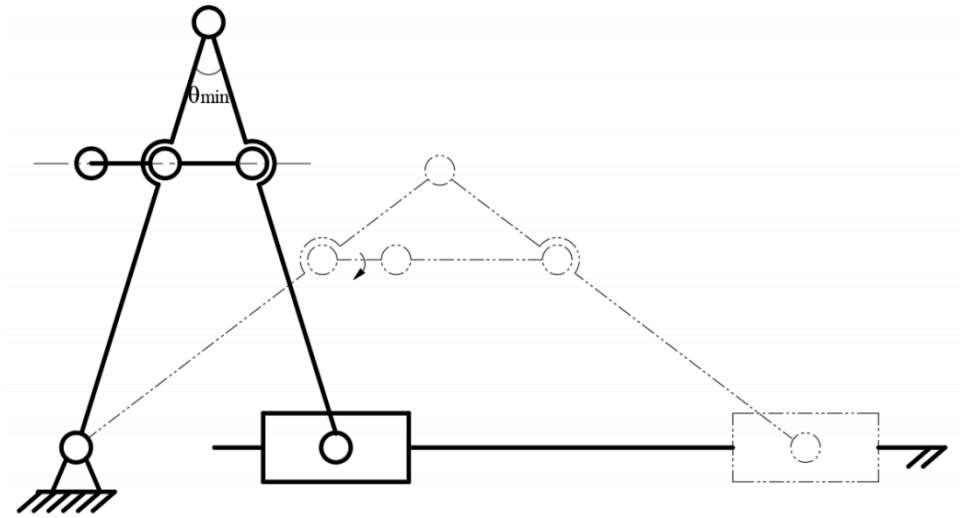


*Figure 3 (a & b). Kinematic Sketch of Forearm and Rear Arm Motion Mechanism[7]*

Kinematic sketches above of the forearm and rear-arm slider–crank mechanism in an inchworm-style climbing robot. The front-arm phase produces forward thrust; the rear-arm phase repositions the body. Analytical results (l = 2bz/a) directly relate crank geometry to stride distance, providing dimensional relationships for the MuJoCo model.

Together, these visuals illustrate the translation of biological principles into engineered mechanisms, bridging the gap between the continuum biomechanics of Manduca sexta and the discrete linkage design required for foldable robotics.

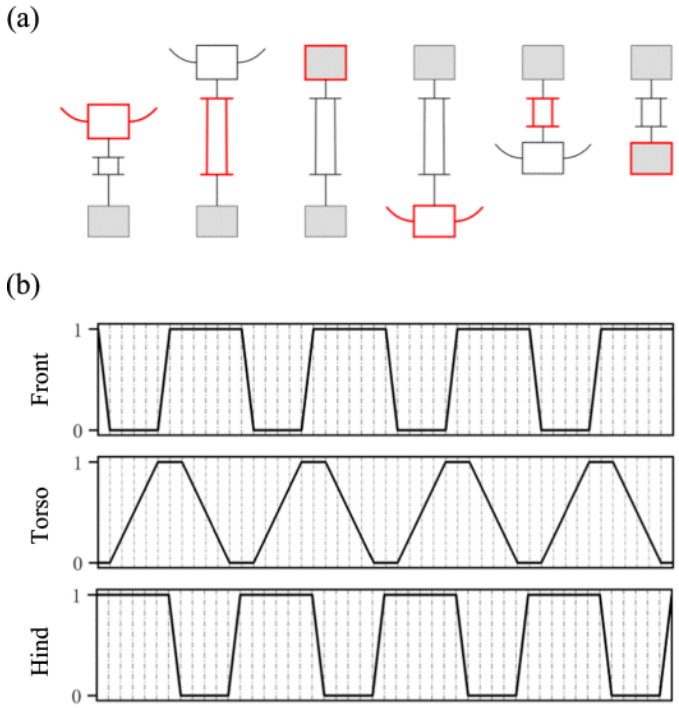


*Figure 4. Gait of the climbing robot. (a) Gait of the motor. (b) Control signals [5]*

The figure above shows two end clamps with a central linear actuator. Shows force path during extension and contraction phases and transition timing diagram (rear on/front off → front on/rear off).

## *2.5. Project Novelty*

The novelty of this project lies in its integration of biomechanical data, parametric simulation, and foldable physical prototyping to systematically study inchworm-inspired locomotion. While prior inchworm robots emphasize soft materials or cable-driven actuation, the approach builds a rigid, foldable linkage crawler whose geometry and friction properties are quantitatively grounded in Manduca sexta biomechanics. Using MuJoCo simulation, the team will vary link lengths, hinge damping, and actuation displacement to evaluate their influence on stride length, lift height, and energy efficiency, establishing analytical relationships between mechanism parameters and gait performance. These findings will then be validated with physical prototypes fabricated from laser-cut laminates, allowing direct comparison between simulated and real motion. This closed-loop workflow linking biological benchmarks, simulation-based optimization, and experimental validation provides a novel framework for

designing biomimetic foldable robots that are both mechanically efficient and analytically traceable.

# 3. Goal Performance Metrics

## *3.1. Design scale and givens*

- Body length, L = 100 mm.
- Target stride, S = 0.25 L = 25 mm.
- Lift, H = 8–10 mm.
- Nominal mass m = 0.05 kg (folded laminate + micro-actuator).
- Gravity g = 9.81 $m/s^2$
- Normal load N = m g = 0.4905 N.
- Friction states: $\mu_{anchor}$ = 0.8, $\mu_{slide}$ = 0.2.

## *3.2. Net thrust and acceleration*

During a half-cycle, one pad anchors (high $\mu$), the other slides (low $\mu$). Net propulsive force is the friction difference on the shared normal load.

With one pad anchored and the other sliding:

$$F_{Thrust} = (\mu_{anchor} - \mu_{slide})N$$
$$= 0.6 \times 0.4905 = 0.294\ N.$$

Instantaneous acceleration (upper bound, inertia included):

$$a = F_{Thrust}/m \approx 0.294 / 0.05 \approx 5.9\ ms^2$$

## *3.3. Speed and duty cycle*

Average speed equals stride per cycle times cycle frequency

$$f = 0.4\ Hz\ (2.5\ s\ per\ cycle).$$
$$v = S f = 0.025 \times 0.4 = 0.010\ m/s = 10\ mm/s$$

## *3.4. Actuator stroke and force*

A linkage maps the actuator stroke to body shortening. Mechanical advantage M A = $s_{act}/\Delta x$ trades stroke for force.

$$\Delta x = S$$

Actuator stroke, $s_{act} = 10\ mm$ via linkage mechanical advantage

$$MA = s_{act}/\Delta x = 10 / 25 = 0.4$$

Required actuator force:

$$F_{act} = F_{Thrust}/MA = 0.294 / 0.4 = 0.74\,N$$

Design target $F_{act} \geq 1.0\,N$ to cover inefficiencies.

### *3.5. Joint torque*

Force applied at radius *r* produces torque. If r = 5 mm,

$$\tau = F_{act} r = 1.0 \times 0.005 = 0.005\,N{\cdot}m$$

Motors with stall torque greater than 0.02 N·m provides a 4× margin.

### *3.6. Work and power per cycle*

Useful mechanical work per stride is thrust times advance. Average power is work times frequency.

$$work = F_{Thrust} S = 0.294 \times 0.025 = 7.4 \times 10^{-3}\,J.$$

At f = 0.4 Hz,

$$P = 0.0074 \times 0.4 = 3.0 \times 10^{-3} W.$$

Electrical input ≈ 0.2–0.5 W (for DC motor).

### *3.7. Pad sizing and pressure*

Contact pressure *p* affects achievable μ.

Pad area with A = 200 mm² = $2 \times 10^{-4} m^2$,

$$p = N / A = 0.4905 / (2 \times 10^{-4}) = 2.45\,kPa.$$

Select pad materials that keep $\mu_{anchor}$, $\mu_{slide}$ near targets at this *p*.

### *3.8. Payload margin*

Added payload raises normal load and available thrust proportionally.

$$Payload = 2\times self\ weight = 0.10\,kgf$$

$$\Rightarrow \Delta N \approx 0.981\,N.$$

$$F_{thrust,payload} = 0.6\,(N + \Delta N) = 0.6 \times 1.47 \approx 0.88\,N$$

$$F_{act} = \frac{F_{thrust,payload}}{MA} = \frac{0.88}{0.4} \approx 2.2\,N$$

### *3.9. Curvature and rigidity*

Limit $\kappa < 0.1\,mm^{-1} = 100\,m^{-2}$.
For h = 2 mm, surface strain

$$\varepsilon \approx \tfrac{1}{2}(h\kappa)^2 = \tfrac{1}{2}(0.002 \times 100)^2 \approx 0.02\ (2\%)$$

Choose $EI \approx 10^{-3}\ N{\cdot}m^2\ for\ < 1\ mm$ sag under $F_{act}$.

### *3.10. Hinge damping and stiffness (MuJoCo)*

Hinge damping

$$b = 0.02\ to\ 0.05\ N{\cdot}m{\cdot}s/rad\ \ (f \le 0.5\ Hz).$$

Compliant joint stiffness

$$k_\theta = 0.2\text{–}0.5\ N{\cdot}m/rad \Rightarrow \theta = \tau/k_\theta < 0.025\ rad\ (1.4°)$$

with $\tau = 0.005\ N{\cdot}m$.

### *3.11. Surface friction targets*

$$\mu_{anchor} \ge 0.7$$
$$\mu_{slide} \le 0.25$$
$$\mu_{anchor} : \mu_{slide} \ge 3:1.$$

In MuJoCo: ($\mu_{slide}$, $\mu_{anchor}$) = (0.2, 0.8); validate thrust via contact impulses.

### *3.12. Geometry back-solves (slider–crank)*

For the inchworm-like slider crank, the stride follows,

$$S = 2\,b\,z\,/\,a$$

Choose a = 30 mm, b = 20 mm

$$z = S\,a\,/\,(2\,b) = 25 \times 30\,/\,40 \approx 18.75\ mm.$$

If packaging limit z ≤ 12 mm, set b = 30 mm ⇒ z ≈ 12.5 mm.

### *3.13. Energy budget and battery*

$$P_{in} \le 0.5\ W$$

For 10 min, t = 600s ⇒ energy ≤ 300 J.
Cell: 3.7 V, 150 mAh ≈ 0.555 Wh ≈ 2000 J usable, ample for the budget
Average current at P = 0.5W,

$$I = P/V \approx 0.14\,A.$$

### *3.14. Cost of Working (partial energy cost)*

Cost of Working (COW) is energy per unit weight–distance. Mechanical lower bound uses useful work; electrical includes losses.

S = 0.025 m
m = 0.05 kg

$$COW_{mech} = \frac{W_{cycle}/S}{m} = \frac{F_{thrust}}{m} * \frac{S}{S}$$

$= \frac{0.294}{0.05*9.81} \approx 5.9\,J/(kg{\cdot}m)$, is normalized by weight.

We can also use $E/m$

$$COW_{mech} = \frac{W_{cycle}}{mS} = 0.0074 \,/\, (0.025 \times 0.05) \approx 5.9\,J/(kg{\cdot}m)$$

### 3.15. Electrical Using Input Power and Speed

With $v$ = 0.01m/sv =0.01 m/s, $P_{in}$=0.2−0.5W:

$$COW_{elec} = P_{in} \,/\, (v\,m)$$

$$COW_{elec} \approx 0.2 \,/\, (0.01 \times 0.05) = 400$$

to $0.5 \,/\, (0.01 \times 0.05) = 1000\,J/(kg{\cdot}m)$

$$COW_{elec} = 400\ to\ 1000\,J/(kg{\cdot}m)$$

# 4. Specifications Table

| Metric | Definition | Target | Usage | Reference |
|---|---|---|---|---|
| Stride length (S) | Horizontal travel per cycle of the four-bar coupler | 10-15 mm | Sets drag-link geometry and crank amplitude | [3] |
| Lift height (H) | Vertical displacement of the Sarrus stage | 2-5 mm | Ensures ground clearance during swing | [5] |
| Cycle period (T) | Time for one lift-and-drag sequence | 1.8-3 s | Determines actuator frequency (0.3 to 0.6 Hz) | [4] |
| Average speed (v) | Net forward velocity | 5-20 mm/s | Benchmark for comparing geometries | [5] |
| Payload (M) | Supported mass of the robot and load | 50-200 g | Used in GRF and torque calculations | [4] |
| Ground-reaction force ($F_n$) | Normal reaction at each pad during stance | 1.5 × W | Input for Jacobian-based torque mapping | [3] |
| Actuator torque ($\tau_{max}$) | Peak motor output during contraction | 0.05-0.1 Nm | Drives power computation $P = \tau\,\omega$ | [4] |
| Energy per cycle (E) | Work required for one stroke | 0.1-0.5 J | Used for efficiency analysis | [3] |
| Friction coefficients ($\mu_a/\mu_s$) | Anchor vs sliding interface values | 0.9 / 0.3 | Determines net displacement $\Delta x$ per cycle | [3] |
| Contact stiffness (k) | Pad compression stiffness | 1.7 N/mm | Defines pad deflection and attachment load | [4] |
| Stroke-length ratio (ΔL/L) | Actuator extension fraction | 0.2–0.3 | Primary independent variable for the study | [3] |

*Table 1: Specifications Table Derived from Literature Review*

- Net displacement ($\Delta x$): measured experimentally and via simulation; indicator of geometric efficiency.
- Velocity–stroke correlation (v vs $\Delta L/L$): used to verify the analytical predictions of [3].
- Power-to-payload ratio (P/M): determines practical scalability.
- Torque and GRF profiles: extracted from the Jacobian for validating link forces during stance.

These metrics will serve as the basis for data collection in the Colab + MuJoCo environment and for comparing different linkage geometries and lift-stroke configurations.

# 5. Mechanism Development

## *5.1. Making of the Mechanism*

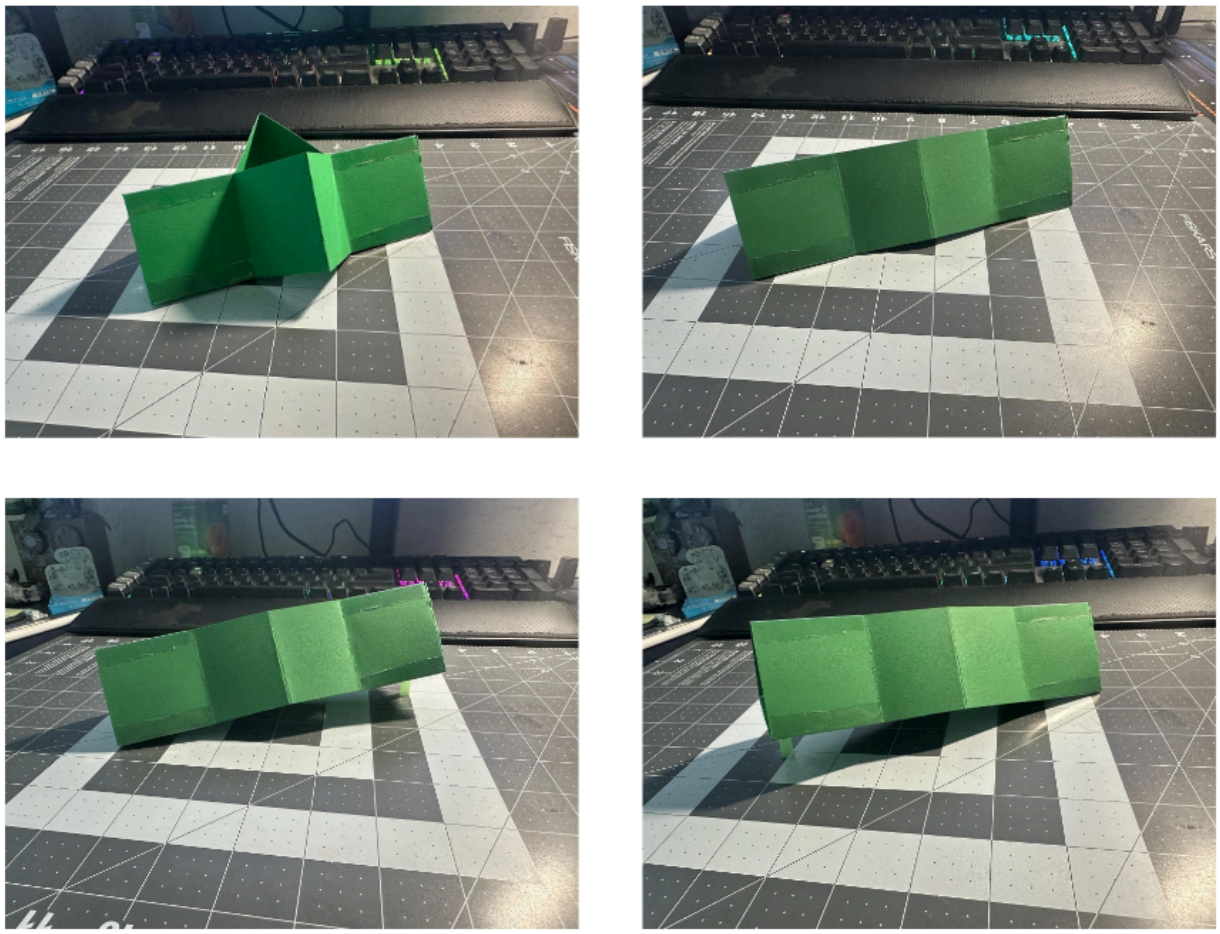

*Figure 5: The four different stages of the inchworm mechanism*

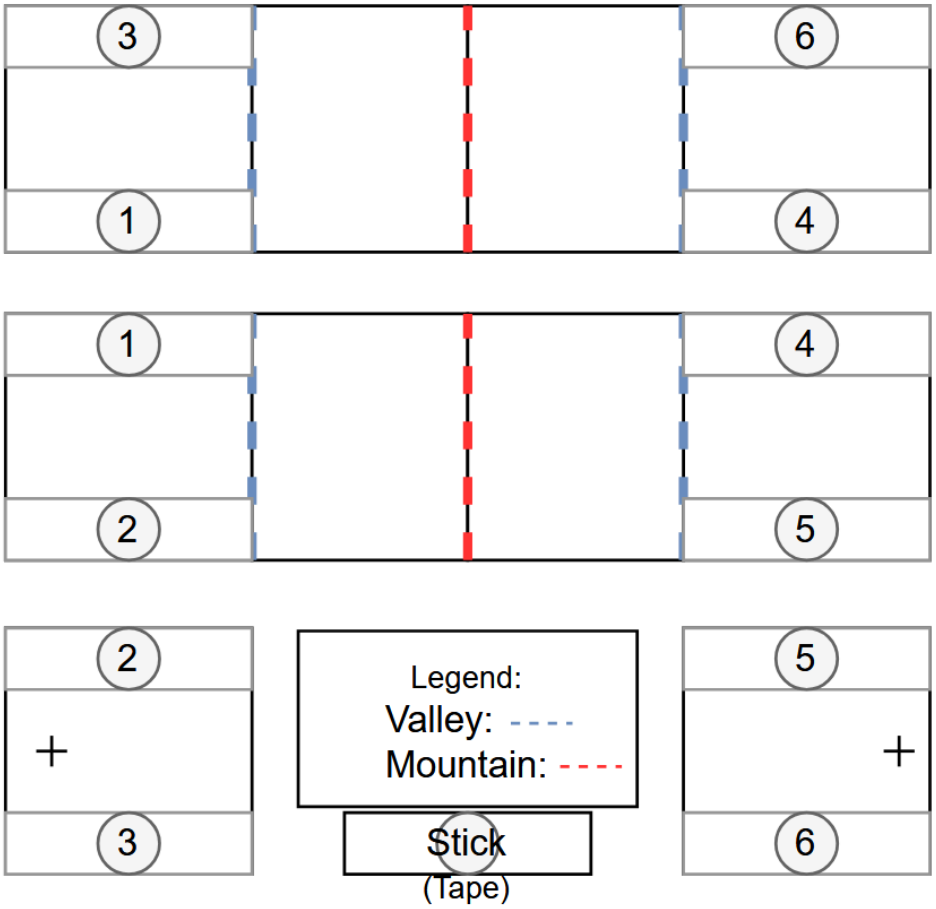


*Figure 6: The cut and fold sheet for the paper prototype*

All sides of the triangle of the mechanism are made of individual pieces of paper and use tape as a joint to connect them all.. This was done to make assembly and rapid changes easier. On the two single squares, holes are poked out to allow for straws to poke through and show vertical lift.

## *5.2. Mechanism Drawing*

Below in Figure 7 below is the simplified version of the team's mechanism represented kinematically. It is shown in both its swing phase and fully extended phase, and how the reference frames react to the change.

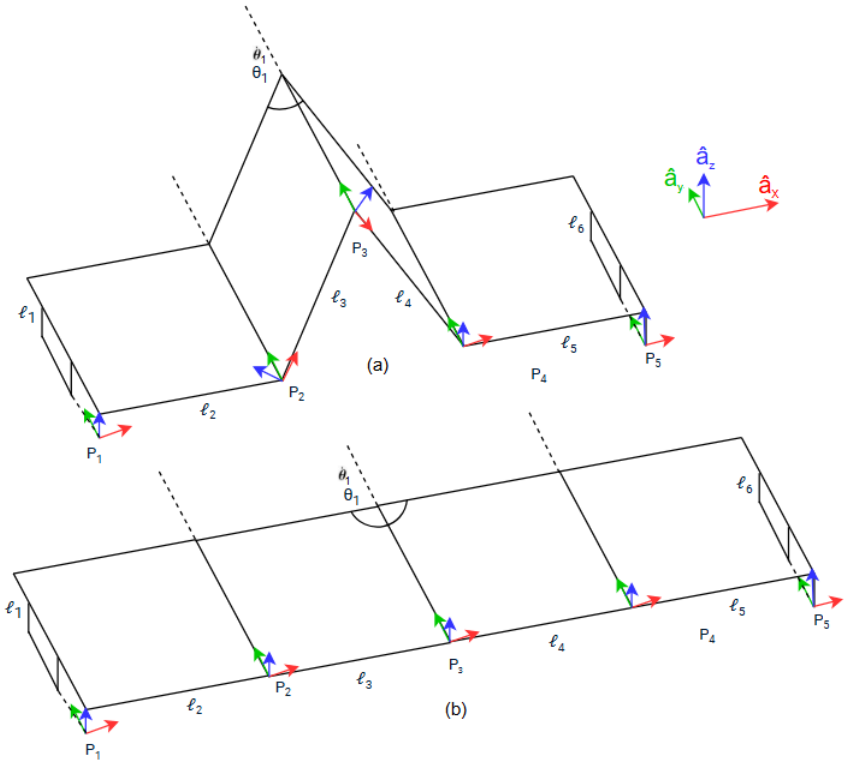


*Figure 7: Simplified Kinematic Diagram of the Proposed Mechanism with a mid swing phase (a), and a fully extended phase (b).*

## *5.3. Next Iteration*

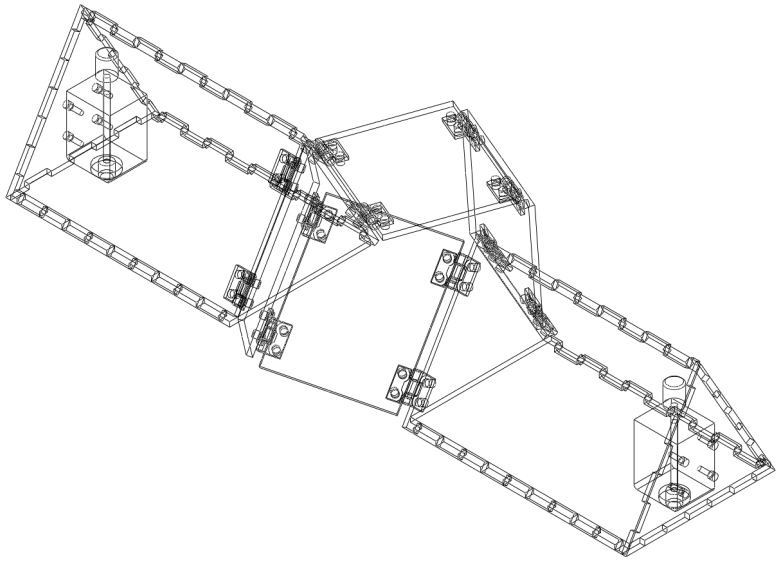

*Figure 8: Detailed skeletalized next iteration.*

The team began a higher fidelity design that implements concrete hardware choices and physical hinge mechanisms, moving from concept to manufacturable detail. This iteration locks the BOM, defines hinge kinematics and tolerances, and integrates mounting and clearance features to enable a buildable, test-ready prototype.

# 6. Kinematic Model

The team went with developing the model in MuJoCo, so most of the work was done via simulation, not analytically or symbolically. Below are snippets of the code where certain requirements were met.

## *6.1. Variable Definition*

The following below is the XML file where the model was created. Each body, joint, and weld was defined here to create an accurate representation of the system.

```
xml = '''
<mujoco>
  <default>
    <light castshadow="false" diffuse="1 1 1"/>
    <camera fovy="45"/>
  </default>
   <!--<option><flag contact="disable"/></option>-->
  <option integrator="RK4"/>
  <option timestep="1e-4"/>
  <option gravity="0 0 -9.81"/>
  <worldbody>
    <light name="top" pos="0 0 2"/>
    <light name="top1" pos="1 0 2"/>
    <light name="top2" pos="2 0 2"/>
    <light name="top3" pos="3 0 2"/>
    <light name="top4" pos="4 0 2"/>
    <camera name="triangle" pos="7 0 .75" euler="90 90 0"/>
    <camera name="iso" pos="-2 -3 3" euler="45 -45 -30"/>
    <camera name="iso2" pos="6 -3 3" euler="45 45 30"/>
    <geom name="ground" type="plane" pos="0 0 -.25" size="5 5 .05" rgba=".5 .5 .5 1"
contype="2" conaffinity="1"/>
    <body name="base_bot" pos="0 0 0" >
      <joint type="free"/>
      <geom type="box" size=".5 .5 .05" pos=".5 0 0" rgba="1 0 0 1" mass="1" contype="1"
```

```
conaffinity="1"/>
      </body>
      <body name="base_left" pos="0 .25 .433" quat=".866 -.5 0 0">
        <joint type="free"/>
        <geom type="box" size=".5 .5 .05" pos=".5 0 0" rgba="1 0 0 1" mass="1" contype="1"
conaffinity="1"/>
        <body name="first_left" pos="1 0 0" axisangle="0 1 0 -45">
          <joint name="first_left" type="hinge" axis="0 1 0" pos="0 0 0" range="-45 45"/>
          <geom type="box" size=".5 .5 .05" pos=".5 0 0" rgba="1 1 1 1" mass="1" contype="1"
conaffinity="1"/>
          <body name="second_left" pos="1 0 0" axisangle="0 1 0 90">
            <joint name="mid_left" type="hinge" axis="0 1 0" pos="0 0 0" range="-90 90"/>
            <geom type="box" size=".5 .5 .05" pos=".5 0 0" rgba=".5 .5 .5 1" mass="1"
contype="1" conaffinity="1"/>
            <body name="tail_left" pos="1 0 0" axisangle="0 1 0 -45">
              <joint name="last_left" type="hinge" axis="0 1 0" pos="0 0 0" range="-45 45"/>
              <geom type="box" size=".5 .5 .05" pos=".5 0 0" rgba="1 0 0 1" mass="1"
contype="1" conaffinity="1"/>
              <body name="tail_bot" pos="0 .25 -.433">
                <geom type="box" size=".5 .5 .05" pos=".5 0 0" rgba="1 0 0 1" mass="1"
quat=".866 .5 0 0"/>
                <body name="end_effector" pos="1 -.375 .2165">
                  <geom type="sphere" size=".1" pos="0 0 0" rgba="1 1 1 1" mass=".00001"
contype="1" conaffinity="1"/>
                </body>
              </body>
            </body>
          </body>
        </body>
      </body>
      <body name="base_right" pos="0 -.25 .433" quat=".866 .5 0 0">
        <joint type="free"/>
        <geom type="box" size=".5 .5 .05" pos=".5 0 0" rgba="1 0 0 1" mass="1" contype="1"
conaffinity="1"/>
        <body name="first_right" pos="1 0 0" axisangle="0 1 0 -45">
          <joint name="first_right" type="hinge" axis="0 1 0" pos="0 0 0" range="-45 45"/>
          <geom type="box" size=".5 .5 .05" pos=".5 0 0" rgba="1 1 1 1" mass="1" contype="1"
conaffinity="1"/>
          <body name="second_right" pos="1 0 0" axisangle="0 1 0 90">
            <joint name="mid_right" type="hinge" axis="0 1 0" pos="0 0 0" range="-90 90"/>
            <geom type="box" size=".5 .5 .05" pos=".5 0 0" rgba=".5 .5 .5 1" mass="1"
contype="1" conaffinity="1"/>
            <body name="tail_right" pos="1 0 0" axisangle="0 1 0 -45">
              <joint name="last_right" type="hinge" axis="0 1 0" pos="0 0 0" range="-45
45"/>
              <geom type="box" size=".5 .5 .05" pos=".5 0 0" rgba="1 0 0 1" mass="1"
contype="1" conaffinity="1"/>
            </body>
```

```
            </body>
          </body>
        </body>
    </worldbody>
    <equality>
        <weld body1="tail_bot" body2="tail_right"/>
        <weld body1="tail_left" body2="tail_right"/>
        <weld body1="base_bot" body2="base_left"/>
        <weld body1="base_bot" body2="base_right"/>
        <weld body1="base_left" body2="base_right"/>
    </equality>
    <actuator>
        <position name="mid_act" joint="mid_left" kp="200" />
        <position name="mid_act2" joint="mid_right" kp="200" />
    </actuator>
</mujoco>
'''
```

The outcome of this definition is a triangular prism with a two-sided single joint mountain fold to achieve the inchworm mechanics, shown below in Figure 9. It has been tested both constrained at its base, as well as with free joints on the surface, but for this assignment, it will interact as though it is constrained at its base.

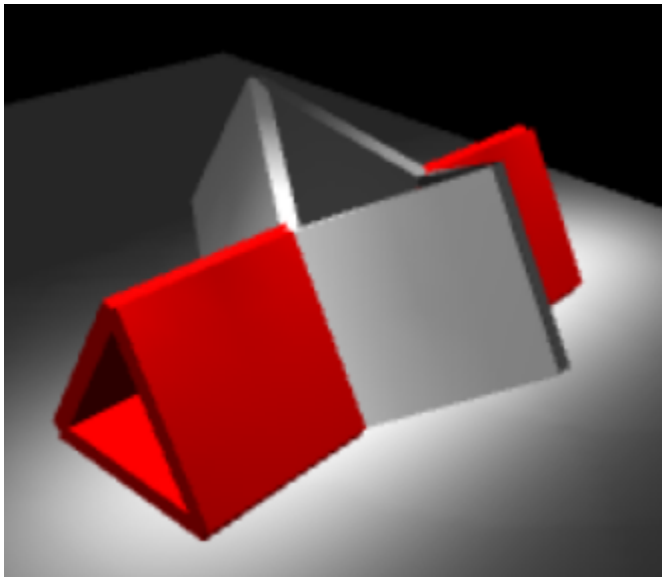

*Figure 9: Inchworm Mechanism*

## 6.2. *Frame Declaration*

The frames and rotations of the system were also defined in the XML above, with each segment being defined as a child of the previous, with rotations created through quaternions.

## 6.3. *Vector Description*

In order to record the position of the mechanism, an alternative angle is shown in Figure 10, with a sphere point representing the end effector. This sphere is a child of the last link in the system, and is placed directly in the middle of the triangle formed by the connected geoms.

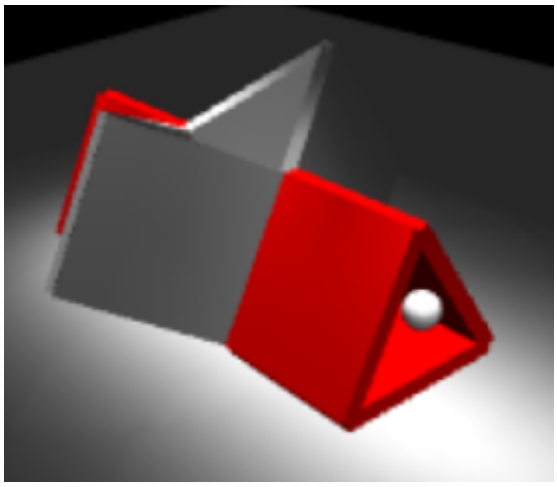

*Figure 10: Alternate angle of the mechanism showing the end effector*

This geom is recorded in the script and then later utilized to calculate the full Jacobian of the system. This is the primary key point within the system, and the only one identified for this simplistic version of the mechanism. Later on down the line, locations such as the friction points on the bottom where the solenoids will create a contact point will also be modeled into the simulation. However, for now, it is just the end effector of the inchworm

```
def get_pos():
    mujoco.mj_forward(model, data)
    return data.body('end_effector').xpos.copy()
```

## *6.4. Phase State Identification*

There are three main states of the system, and those are fully contracted, in-swing, and fully extended. These were chosen at this stage of development due to the mechanism's simplicity. It can only do one motion, and that motion is broken up into three previously identified states. However, in the future, there will be more stages to the gait of the system, akin to those found in the background research, like anchoring on either side of the fold to allow the inchworm to move using friction to keep it from sliding.

## *6.5. State Plotting*

Below are the plots of the identified states of movement simulated in MuJoCo. The states can be categorized by the rotation value of the middle joint, as that is the primary independent variable at this stage in development. When the inchworm is fully extended, the middle joint is not actuated. During its swing phase, the middle joint's rotation is a range between one and one hundred seventy-nine degrees. And finally, its fully contracted state results in a middle joint rotation of one hundred eighty degrees.

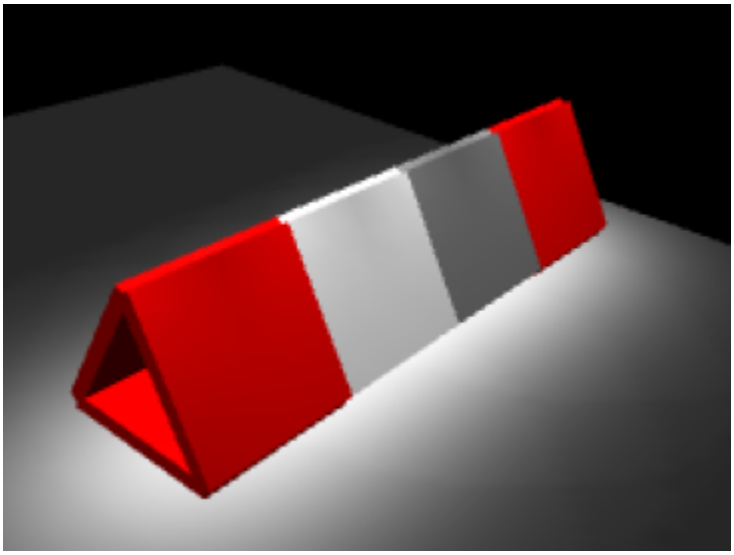

*Figure 11: Mechanism fully extended*

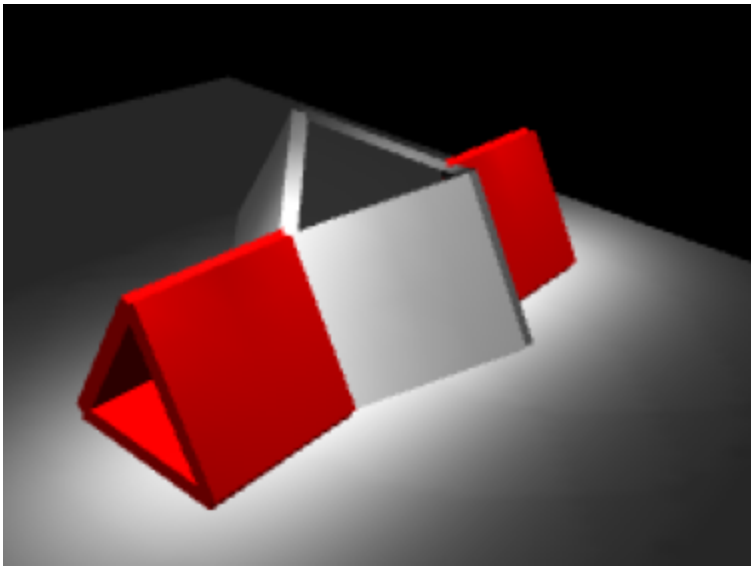

*Figure 12: Mechanism in-swing*

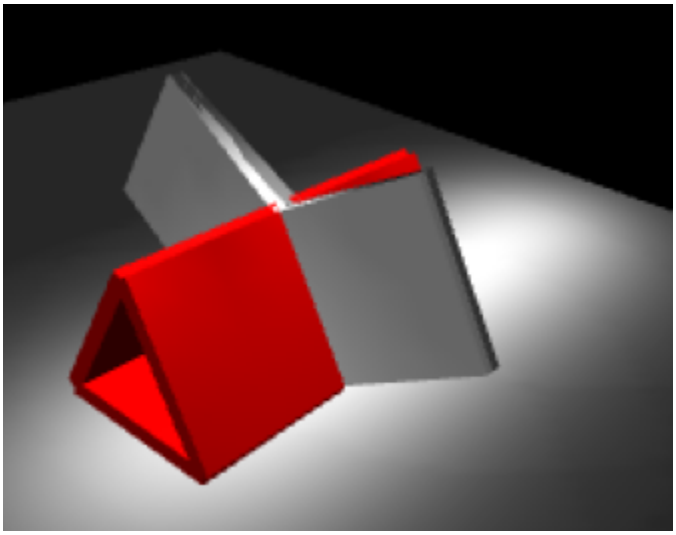

*Figure 13: Mechanism fully contracted*

## *6.6. Jacobian Creation*

The Jacobian for this system was defined with the only key joint in mind, the middle hinge. Even though there are two hinges, they are symmetrical, and thus can be described the same using a 3x1 Jacobian matrix, shown below, calculated iteratively using end effector position data. The calculation for the Jacobian is also displayed below in the code snippet.

```
Numerical Jacobian:
 [-1.12727141 -1.18876712 -0.68629475]
```

```
n = model.nv

def get_pos():
    mujoco.mj_forward(model, data)
    return data.body('end_effector').xpos.copy()

# Initialize
J_numeric = np.zeros((3, n))
dq = 1e-4  # small perturbation

for i in range(n):
    q_backup = np.copy(data.qpos)

    # Forward position
    x0 = get_pos()

    # Perturb one joint
    data.qpos[i] += dq
    mujoco.mj_forward(model, data)
    x1 = get_pos()

    # Compute derivative
    J_numeric[:, i] = (x1 - x0) / dq

    # Restore
    data.qpos[:] = q_backup
```

- Force Relationships

  To understand the force relationship of the system, the GRF must first be estimated to give the Jacobian a way to calculate the torque on the joint. In the background research, it was found that an accurate estimation was 1.5x the weight of the model [3] in the z direction. The team decided on a goal weight of .05kg, which would make the GRF 9.81*1.5*.05 = 0.736N. Applying this to the Jacobian yields:

  ```
  Torque on middle joint:  [-0.50494136] Nm
  ```

- Velocity Relationships

  From the specifications table, it is found that a nominal net forward velocity is anywhere between 5-20 mm/s [5]. The team will use 10 mm/s as a goal for these calculations. To achieve this motion, the middle joint

will need to move according to this sinusoidal frequency found iteratively through guess and check:

```
A = np.deg2rad(45)   # amplitude: 30 degrees
freq = .35           # Hz
omega = 2 * math.pi * freq
```

Applying this function to the middle joint and running the calculations, the output end effector velocity is:

```
End effector velocity:  [0.01188584 0.04381576 0.02529556] m/s
```

## *6.7. Power Computation*

| Part | Qty | Voltage | Max amp | Max Watt | Total Watt |
|---|---|---|---|---|---|
| ESP32-DEVKITC-32 UE (1965-ESP32-DEVKI TC-32UE-ND) | 1 | 3.3 | 0.239 | 0.789 | 0.789 |
| Pololu 3042 Gearmotor 12V (2183-3042-ND) | 1 | 12.0 | 0.72 | 8.64 | 8.64 |
| Adafruit 413 Solenoid 12V (1528-1552-ND) | 2 | 12.0 | 1.0 | 12.0 | 24.0 |

*Table 2: Power Budget*

The team is assuming 100% usage to follow worst-case design practice, verify the system meets requirements at the extreme operating/environmental limits, not just at “typical,” so margins are real and failures are unlikely.

## *6.8. Discussion*

- Degrees of Freedom

This system can have a few different degrees of freedom, depending on how the model is defined. For example, in the MuJoCo

model, there are plenty of joints that define the mechanism, but also many constraints. Thinking about it logically, the only direction the system can go is along the x-axis, so it makes sense that the total degrees of freedom are one. However, the model also uses two actuators to drive that movement. They are placed as mirror versions of themselves, so the action is symmetrical. This could either mean that the total DoF is one or two, depending on how one looks at the system as a whole.

This answer will also change once the model has developed the contact points, as those actuate themselves and add a degree of freedom each. Also, once the system isn't constrained at its base, but instead free to move in real space, that adds other degrees of freedom in rotation and world position.

Regardless, the most logical and simplistic explanation is that this inchworm has one DoF, using the middle joints to actuate in the x-axis direction.

- End-Effector Forces

The team estimated the end effector forces via referencing background research on similar mechanisms, settling on a resultant GRF of 1.5x [3] the weight of the system, which was also a goal to set at 0.05kg [4]. After computing with the Jacobian, the torque on the mid joint was determined. Defining the relationship between the force on the system and the experienced torque helps consider how much load can be placed on the mechanism and how it will react. The total forces acting on the system will change as the model develops, when other aspects like friction come into play, but that is for a later time.

- End-Effector Speeds

Branching off the target gait frequency and stride of the mechanisms found in literature, a frequency of .35 Hz [4] was used to find the end effector velocities, which were also set at a target goal of 10mm/sec [5]. The calculated end effector cartesian velocity did end up having 10mm/sec in the x-axis direction; however, it also had extraneous velocities in the other directions that need to be worked out in the future.

# References

[1] L. I. van Griethuijsen and B. A. Trimmer, “Kinematics of horizontal and vertical caterpillar crawling,” *J Exp Biol*, vol. 212, no. 10, pp. 1455–1462, May 2009, doi: 10.1242/jeb.025783.

[2] H. T. Lin and B. A. Trimmer, “The substrate as a skeleton: ground reaction forces from a soft-bodied legged animal,” *J Exp Biol*, vol. 213, no. 7, pp. 1133–1142, Apr. 2010, doi: 10.1242/jeb.037796.

[3] R. H. Plaut, “Mathematical model of inchworm locomotion,” *International Journal of Non-Linear Mechanics*, vol. 76, pp. 56–63, Nov. 2015, doi: 10.1016/j.ijnonlinmec.2015.05.007.

[4] W. Wang, K. Wang, and H. Zhang, “Crawling gait realization of the mini-modular climbing caterpillar robot,” *Progress in Natural Science*, vol. 19, no. 12, pp. 1821–1829, Dec. 2009, doi: 10.1016/j.pnsc.2009.07.009.

[5] R. Li *et al.*, “An Inchworm-Like Climbing Robot Based on Cable-Driven Grippers,” *IEEE/ASME Transactions on Mechatronics*, vol. 29, no. 2, pp. 1591–1600, Apr. 2024, doi: 10.1109/TMECH.2023.3307682.

[6] M. Pan *et al.*, “Bioinspired Mechanisms and Actuation of Soft Robotic Crawlers,” *Advanced Science*, vol. 12, no. 16, p. 2416764, 2025, doi: 10.1002/advs.202416764.

[7] W. Fan, “A Kinematic Analysis of a Line Robot Based on Biomimicry of Inchworms,” *IJFET*, vol. 6, no. 3, 2024, doi: 10.25236/IJFET.2024.060311.